Original Article

Antimicrobial activity and physicochemical characterization of thermoplastic films based on bitter cassava starch, nanocellulose and rosemary essential oil

Josette Araya[1], Marianelly Esquivel[1], Guillermo Jimenez[1] (iD)**, Diana Navia[2] and Luis Poveda[2]**

Abstract

Extended shelf-life of many foods is a modern requirement that has been achieved by means of fossil-based plastic films despite their environmental issues. Recently, starch-based, fully biodegradable thermoplastics are gaining momentum as packaging material; however, if they are in contact with food, aspects such storage, water interaction and spoilage due to microorganisms must be considered. Essential oils are of great interest due to their antimicrobial action, so incorporating these compounds into natural polymers can promote a longer shelf life through active packaging. In this study, antibacterial activity, optical, mechanical and barrier properties of thermoplastic starch (TPS) films based on cassava starch (*Manihot esculenta Crantz*) and rosemary essential oil (REO) were studied. Furthermore, the effect of cellulose nanocrystals (CNC) on TPS properties were surveyed. Film mechanical properties and those related to the interaction with water, showed that the highest resistance and barrier properties corresponded to the TPS/CNC 15% film, while adding oil to the films increased

[1]Polymer Laboratory, School of Chemistry, Universidad Nacional, Heredia, Costa Rica
[2]Grupo de Investigación Biotecnología, Facultad de Ingeniería, Universidad de San Buenaventura Cali, Cali, Colombia

Corresponding author:
Guillermo Jimenez, Polymer Laboratory, School of Chemistry, Universidad Nacional, Heredia, Costa Rica.
Email: gjime@una.ac.cr

morphological heterogeneity, contributed to reduce tensile strength, and increased water solubility and water vapor permeability. Likewise, TPS films containing rosemary oil showed enhanced antibacterial activity mostly against *E. coli* and *S. aureus* bacteria and *A. niger* fungus. Therefore, adding essential oils as natural additives favors using these biocomposites as functional packaging, and as potential replacements for single-use plastics.

Keywords
Essential oil, rosemary, thermoplastic starch, cellulose nanocrystals

Introduction

In response to environmental concerns caused by the disposal of synthetic polymeric materials derived from non-renewable resources, researchers have focused on developing bio-based plastics, such as those using polysaccharides. Polysaccharide films, such as starch, have been a topic of extensive research, as this raw material can be obtained from agricultural sources, making it renewable, inexpensive, widely available and easy to handle.[1]

Cassava starch has been widely used to produce films, with results showing that these carbohydrates are promising materials.[2–6] Films developed from starch are described as isotropic, odorless, tasteless, colorless, non-toxic, and biodegradable.[7] However, applying native starches to produce films is limited due to their hydrophilic nature, which leads to films with poor mechanical properties and water resistance.[7–9]

Various strategies have been adopted to improve water resistance of starch-based films, including incorporating cellulose in the thermoplastic starch (TPS) matrix, which also might act as a reinforcing material without affecting its biodegradability.[10] In this regard, nanocrystalline cellulose (CNC) has been used as an ecological filler and reinforcement for biopolymers due to its low cost, wide availability, renewability, biodegradability and safety.[11] CNC is usually prepared by acid hydrolysis of the cellulose, which removes its amorphous regions, resulting in particles essentially formed by crystalline structures.[12]

Utilizing CNC as reinforcement material for thermoplastic starch, seems particularly interesting given the chemical similarities in the structure of both polysaccharides. Additionally, there is the possibility of hydrogen bonding between both components, resulting in good adhesion at the matrix/filler interface, and avoiding coupling or surface agents. Several findings by Babaee,[13] Kalia,[14] and González[15] have reported on the reinforcement of starch-based materials with cellulose nanofibers, nanocrystals and nanowhiskers. According to these studies, starch-based materials showed enhanced mechanical properties, and moisture resistance upon adding nanocellulose.

Oriani,[2] Khalid,[16] and Luchese[17] added essential oils to the TPS thermoplastic matrix to provide functional properties to the films. Essential oils are aromatic, volatile, and natural liquids extracted from different parts of plants such as flowers, seeds, leaves, and stems.[18–20] The composition and physicochemical properties of the essential oils are highly influenced by the species, part(s) of plants used, geographic origin, harvest time, stage of development, age of plants and extraction method.[21,22] They are considered natural hydrophobic additives, and are often used to protect food against oxidation and microbial spoilage.[23,24] Active packaging provides microbial safety for consumers by reducing, inhibiting, or delaying the growth of microorganisms, which might extend the shelf life of packaged foods.[25–29] In this regard, several essential oils have been tested as functional components to formulate starch films with antimicrobial properties such as those reported by Avila-Sosa,[30] Ghasemlou,[31] Amaral,[32] De Sousa,[33] and Rajaei.[8] Rosemary essential oil (REO) has shown acceptable results in terms of antimicrobial efficacy, when incorporated into thermoplasticized starch films from different plant sources.[8,32] In addition, Castaño,[34] Montero-Recalde,[35] and Jiang[36] reported that REO shows antibacterial activity against gram-positive bacteria (*Staphylococcus epidermidis, Staphylococcus aureus* and *Bacillus subtilis*), gram-negative bacteria (*Proteus vulgaris*, *Pseudomonas aeruginosa* and *Escherichia coli*), and fungi (*Candida albicans* and *Aspergillus niger*). Based on this context, the minimum inhibitory concentration (MIC) of REO for three bacteria and three fungi were established in this work. Then, REO was incorporated into the formulation of TPS and TPS/CNC thermoplastic starch films. Our main goal was to develop active compound films, and to verify the effect that the added REO has on the mechanical and barrier properties of the films, as well as on the antimicrobial activity against fungi and bacteria commonly found in food.

Materials and methods

Materials

Bitter cassava starch *(Manihot esculenta Crantz)* was used, (CIAT-coded CM7951-5 variety), harvested in the North-Caribbean region of Costa Rica. Such starch variety shows 76.7 wt.% total starch content, 21 wt.% amylose, and a gelatinization temperature of 77°C, as determined by differential scanning calorimetry (DSC). CNC was obtained using an acid hydrolysis method described by Dos Santos[37] on pineapple green leaves (*Ananas comosus*) from the Northern Caribbean region of Costa Rica. Rosemary (*Romerus officialis*) oil was purchased at the local market in the city of Cali (Cauca Valley, Colombia). Reagent grade chemicals such as sodium hydroxide, hydrochloric acid, sodium chlorite and sulfuric acid were purchased from Fischer Scientific (PA, USA).

Microorganisms. Microbial cultures were collected from the American Type Culture Collection (ATCC) at the University of San Buenaventura, in Cali, Colombia.

One gram-positive bacteria *Staphylococcus aureus* ATCC 55804, and two gram-negative bacteria, *Salmonella enteric* ATCC 53648 and *Escherichia coli* ATCC 11,775 were evaluated. Also, three strains of fungi, namely, *Aspergillus niger, Aspergillus flavus* and *Fusarium oxiporum* were used. For the microbiological analysis, Müller Hinton agar (MH) (Oxoid®) and potato dextrose agar (PDA) for fungi were utilized. The bacterial cultures and fungi were previously activated and incubated at 25°C and 37°C.

Methodology

Rosemary oil extraction. REO was extracted using the hydrodistillation method.[38] Plant leaves and thin stems were placed in distilled water (mass/volume ratio 1/12) and REO was extracted in an hydrodistillation system for 3 hours at 100°C. The essential oil was then stored under refrigeration at 10°C in an amber glass bottle.

Characterization of REO by gas chromatography–mass spectrometry. The analysis of the components present in the extracted REO was carried out in a gas chromatography–mass spectrometry (GC-MS Thermo Scientific TSQ9000) by the Natural Products Research Center (CIPRONA) at the University of Costa Rica (UCR), located in San Jose, Costa Rica. Data were obtained at 260°C on a TG-5MS 0.25 mm ID Thermo Scientific column, and NIST14, Wiley 11th Ed., Wiley FFNSC 3 libraries.

Quantification of total phenols in REO. The total phenol content was assessed according to Erkan.[39] A 0.1 mL aliquot of equivalent gallic acid was mixed with 0.5 mL of absolute ethanol, and aqueous dilutions at 100, 50, 25 and 12.5% v/v were prepared. Subsequently, 0.1 mL aliquot of each dilution was taken and treated with 0.250 mL of Folin-Ciocalteu reagent (Sigma-Aldrich), prepared in a 1:1 reagent-distilled water ratio. After allowing it to stand for 5 minutes at room temperature, 1.25 mL of 20% aqueous sodium carbonate solution was added. Solutions remained protected from light for two hours, then absorbance was measured on a spectrophotometer (Thermo Electron Corporation) GENESYS 10 UV at 760 nm, using ethanol blank. Quantification was based on the standard gallic acid curve, and the results were expressed in milligrams of gallic acid equivalents (GAE) per gram of sample (mg GAE per gram of sample). Measurements were done in triplicate.

Extraction of cellulose nanocrystals. Isolated cellulose from pineapple leaves (PAL) was subjected to hydrolysis with sulfuric acid (64 wt.%), with vigorous agitation for 2 hours at 45°C. Then, reaction was quenched with cold water, centrifuged twice for 10 minutes and 7000 rpm, dialysis was carried out until neutral pH, and finally 10 minutes of sonication was applied before storing at 4°C.

Characterization of cellulose nanocrystals. Transmission electron microscopy (TEM) and dynamic light dispersion (DLS) were utilized to characterize CNC extracted

from PAL. TEM survey (Hitachi HT7700, 100 kV) was carried out at the Microscopic Structures Research Center (CIEMIC), UCR, San Jose, Costa Rica. DLS data (Zetasizer Ultra, Malvern Panalytical) were obtained at the School of Chemical Engineering, UCR, San Jose, Costa Rica.

Preparation of thermoplastic starch films. Films were produced by the casting method, that is, evaporation of the solvent at controlled temperature and humidity. Preparation of the thermoplastic starch films was carried out according to a compilation of methods and compositions established by Luchese,[17] López,[40] and De Sousa.[33] Film compositions are shown in Table 1.

In order to prepare the films, starch and glycerol were added in water and mixed for 10 minutes at room temperature. The film-forming solutions were then heated at 90°C until reaching gelation temperature; CNC was added and stirring continued for 15 min without heating. After cooling at 40°C, Tween 80® was added in a 50 wt.% proportion with respect to REO, followed by the incorporation of the essential oil to the film-forming solution, and homogenization in an Ultra Turrax T-25 D Homogenizer at 1000 rpm for 2 min. Then, the solution was cooled down in an ultrasound bath for 1 hour to remove bubbles. Later, $0.25 \, g/cm^2$ of the filmogenic solution was placed in a Petri dish and dried at 40°C for 6 hours inside a forced air convection oven (ESCO OFA-110–8). Finally, films were stored 15 days at 21°C ± 1°C and 55% ± 5% RH for further analysis.

Characterization of the films

Infrared spectroscopy (FT-IR). In order to characterize the films, Fourier Transform Infrared Spectroscopy (FTIR) was carried out with a Thermo Scientific Nicolet iS-50, and according to Ghanbari.[41] Infrared spectra were collected on each of the films, scanning from $4000 \, cm^{-1}$ to $500 \, cm^{-1}$. Samples were analyzed using the attenuated total reflection (ATR) accessory.

Table 1. Composition (wt. %) of the TPS composite films.

Film	Starch (starch/solution)	Glycerol (glycerol/starch)	CNC (CNC/starch)	REO (REO/solution)	Tween 80 (Tween 80/REO)
TPS 20 %	4	20	N/A	N/A	N/A
TPS/CNC 15 %	4	20	15	N/A	N/A
TPS/REO 0.4%	4	20	N/A	0.4	50
TPS/REO 0.5%	4	20	N/A	0.5	50
TPS/CNC/REO 0.4 %	4	20	15	0.4	50
TPS/CNC/REO 0.5 %	4	20	15	0.5	50

N/A: not applicable.

Thermogravimetric analysis (TGA). To determine the thermal stability of the films, thermogravimetric analysis was conducted with a TA Instruments TGA Q500, and according to Ghanbari.[41] Samples were heated up to 800°C at 20° C/min, and under nitrogen atmosphere. Measurements were performed 15 days after the thermoplastic films were prepared.

Differential scanning calorimetry (DSC). Behavior of the films thermal transitions was assessed according to the parameters established by Savadekar.[42] The test was carried out using a Perkin Elmer Pyris DSC-6 under nitrogen gas atmosphere. Samples (6–10 mg) were placed and sealed in aluminum capsules and scanned from 30°C to 300°C at a heating rate of 10°C/min. Measurements were done 15 days after the thermoplastic films were prepared.

Mechanical properties. Mechanical properties of the compounds, such as tensile elastic modulus, percentage of deformation and tensile strength, were determined according to the ASTM D882 standard,[43] and using an Instron 3365 universal testing machine. Rectangular pieces (50 mm × 10 mm) of the films were used and stretched with a crosshead speed of 10 mm/min, and 1 kN load cell. The test was carried out 15 days after preparing the films, at a temperature of 21°C and 70% ± 5% RH. Reproducible data were taken from five specimens of each composition, and the results were presented as an average.

Water solubility. Water solubility of the films was established by the degree of mass lost from samples upon being immersed in distilled water, as described by Ma.[44] The analysis was completed 15 days after the thermoplastic films were prepared. Prior to the immersion, drying at 105°C during 24 hours for each of the films (40 mm × 20 mm, approximately) was applied. Once films were dried, a mass between 100 and 150 mg of the dried film was measured as initial mass (W_0). Sample was then immersed in 30 mL of distilled water and stirred for 24 hours at 90 rpm in an orbital shaker. Once this period was finished, samples were recovered and dried again at 105°C for 24 hours to determine material content not dissolved in water (W_t). Solubility of the film in water was calculated using the following formula:

$$\% \text{ water solubility} = \frac{(W_0 - W_t)}{W_0} \cdot 100 \qquad (1)$$

where:

w_o	=	mass of the dried sample prior to immersion
w_t	=	mass of the insoluble materials after immersion

Water vapor permeability and transmission rate. Water vapor transmission rate was determined gravimetrically following the E96/E96M-16 method (ASTM, 2016), with some of the modifications made by Babaee.[13] Samples were set up in an environmental chamber at 25°C and 70% RH. Five grams of silica gel (0% RH) was added to the circular stainless-steel permeation cell, and a 5.5 mm diameter film sample was fixed on it. The cell was stored in a glass desiccator containing a saturated sodium chloride solution (70 ± 2% RH) at 21°C. The water vapor transmission rate (WVTR) and the water vapor permeability (WVP) were calculated using the following equations:

$$WVTR = \frac{\left(\frac{G}{t}\right)}{A} = \frac{slope}{area} \qquad (2)$$

where

G	=	mass change (g)
t	=	time (h)
A	=	area (m^2)
G/t	=	slope obtained from mass gain vs. time

$$WVP = \frac{WVTR}{P(R_1 - R_2)} \cdot X \qquad (3)$$

where

X	=	film thickness (m)
P	=	saturation vapor pressure of water at 25°C (Pa)
R_1	=	relative humidity in the desiccator (70% RH)
R_2	=	relative humidity inside the cell (0% RH)

Opacity. The opacity was determined following the methodology described by Daudt.[45] The opacity test was performed using a colorimeter, samples (20 mm × 100 mm) were cut from the films, prepared and placed under the measuring opening of the equipment. The opacity was calculated by establishing the relationship between the black standard (Opb) and the white standard (Opw) as references. Data was processed using Spectra Magic NX software, where an average of five measurements for each film was determined at random positions.

Qualitative determination of the minimum inhibitory concentration (MIC). The minimum inhibitory concentration was assessed by the agar dilution method,

which defines the antimicrobial susceptibility against bacteria and fungi.[7] The agar dilution procedure was carried out by inoculation on agar plates, containing the test compound at concentrations of 0, 1000, 2000, 3000 and 4000 ppm of REO on each disk. The antimicrobial agent inhibits growth of the test microorganism, diffusing into agar; results are expressed based on the diameters of the inhibition growth zone. The bacterial cultures (*S. aureus, S. entererica* and *E. coli*) and fungal (*A. niger, A. flavus* and *F. oxyporum*) were adjusted to a concentration higher than 10^6 CFU/mL measured in a Neubauer chamber. The bacterial inoculum was seeded with sterile glass loops on the surface of Müller Hinton agar in Petri dishes, containing the antimicrobial agent at the above concentrations. Fungi were scattered using a circular cutter and placing the sample in the center of the Petri dish containing PDA agar with the antimicrobial agent at the above concentrations. Plates were incubated at 37°C for the quantification of the bacterial colonies at 25°C, for fungi in darkness for 72 hours to determine formation of inhibition zones.[46]

   Qualitative disk inhibition test. Determination of the antimicrobial activity was accomplished using the disk inhibition method.[47] Müller Hinton agar was prepared, placed in Petri dishes, and 0.1 mL aliquots of the bacterial cell suspensions (*S. aureus, S. enterica* and *E. coli*) were inoculated, and adjusted to a concentration > 10^6 CFU/mL in a Neubauer chamber. Subsequently, 0.1 mL of the bacterial inoculum was scattered with sterile glass loops on the agar surface to diffuse its growth. Afterward, a 5 mm disk of each of the prepared films was placed to determine the antifungal effect by visualizing fungal growth zone of inhibitions around the thermoplastic film, in darkness, and 24 hours after incubation at 37°C.

   Determination of the antifungal activity required the preparation of 0.1 mL spore suspensions (*A. niger, A. flavus* and *F. oxyporum*), which were produced taking a section of the sporulated fungal culture and placing it in distilled water; then a concentration > 10^6 CFU/mL was established in a Neubauer chamber. Then, 0.1 mL of the fungal suspension was placed in Petri dishes and dispersed on the surface using sterile glass loops. Finally, a 5 mm disk of each of the films prepared was used to determine the antifungal effect, by monitoring the fungal growth zone of inhibitions around the thermoplastic film, 24 hours after incubation and at 25°C in darkness. In both procedures, monitoring of each bacteria and fungus was accomplished using the same technique, but without the addition of thermoplastic films. The analysis was completed in duplicate for each of the films, and each bacteria or fungus surveyed.

Results and discussion

Characterization of the rosemary essential oil

The hydrodistillation process produced 2.5% extraction yield from dry material made up of leaves and thin stems. The extraction yield through hydrodistillation has been reported as 2.05% and 1.9% for related investigations by Jiang[36] and Özcan,[48] respectively. REO was analyzed by means of gas chromatography coupled

to mass spectroscopy, yielding a total of 38 components (main components are shown in Table 2). Similar works on REO report a total of 22 identified components, with 1,8-cineole (26.54%), α-pinene (20.14%), camphor (12,88%), camphene (11.38%) and β-pinene (6.95%) as the main compounds.[35] In addition, Jalali-Heravi[49] agree with some of the major components determined in this work, such as 1,8-cineole (23.47%), α-pinene (21.74%), verbenone (7.57%), camphor (7.21%) and eucalyptol (4.49%). The volatile fraction of *R. officinalis* differs in compounds and their abundance, depending on the chemotype; differences may probably be due to the environment, genetics, and the nutritional condition of each type of plant.[48]

In this study, the total phenolic content of the rosemary plant extract was 6.71 mg GAE. Meanwhile, studies by Proestos[50] and Hesenov,[51] showed a phenol content of 8.5 and 10 to 36 mg GAE, respectively. On the other hand, storage conditions in Hesenov work indicated that the greatest antioxidant activity occurs at 4°C, in darkness, and with a fresh extract. Therefore, Hesenov proved there is a reduction on the antioxidant effect in REO stored for long time and at high temperature, due to the oxidative destruction of β-carotene by the oxidative degradation of linoleic acid.[51] From those results, it can be highlighted that there is a correlation between the antioxidant activity and the total phenolic content in plants (Lamiaceae family members are very rich in polyphenolic compounds). Differences in volatile oil composition and total phenol content in REO could be attributed to the effects of climate on plants growing in different habitats. In addition, harvest time and distillation type affect the qualitative composition of the volatile oil produced and its storage.[52]

Characterization of CNC

In our present case, although nanosized structures were clearly seen in TEM pictures (see Figure 1), also microsized entities could be observed. This fact was

Table 2. Main components of the rosemary essential oil as obtained by GC-MS.

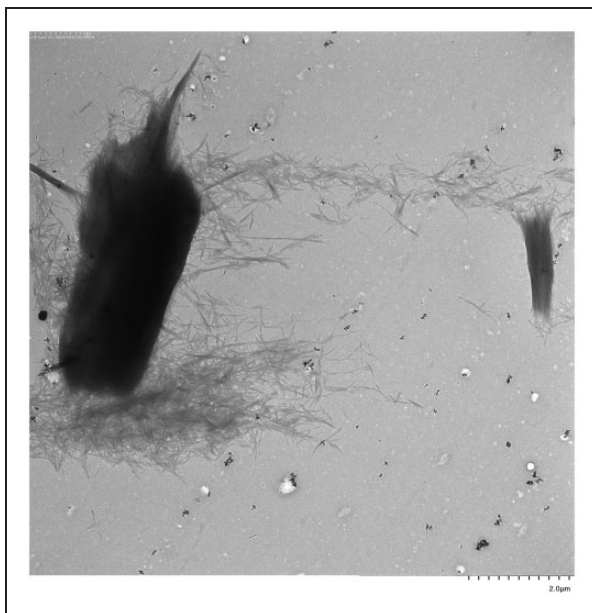| Component	Percentage (%)
Eucalytol	25.23
Camphor	18.39
β-Myrcene	18.14
α-Pinene	10.5
Camphene	4.6
Bornyl acetate	3.54
β-Pinene	3.40

Figure 1. TEM photo (x3k) of cellulose nanocrystals.

corroborated through DLS measurements, in which three main CNC size ranges could be determined; 401–495 nm (51% of the particles per milliliter), 702–807 nm (42%), and 3759–5331 nm (5%). Therefore, it can be considered in this work that a mixture of CNC sizes could be attained, with approximately 95% of the structures in the nanometer scale.

Characterization of the thermoplastic films

Fourier transform infrared spectroscopy (FT-IR). FT-IR spectroscopy was used to investigate changes in the starch structure converted into TPS films at a short-range molecular level, and to identify possible interactions between starch, plasticizer, and additional materials such as CNC and REO. FTIR spectra of the films are shown in Figure 2.

Films having CNC, REO or a combination of both components, presented similar IR signals in terms of their frequency values; however, peak height ratios at 1637 cm^{-1}, 1330 cm^{-1} and 3290 cm^{-1}, (related to the amount of bound water), differed slightly. As it can be seen, these bands widened for samples containing glycerol in comparison to neat native starch, mainly due to the hydrogen bonding interaction between glycerol (R-O-R) and starch (–OH) groups. Nevertheless, a decrease in peak height at 3290 cm^{-1} occurred in materials containing CNC, REO or a combination of both, which might be related to a decrease in the water interaction, as a result from the decrease in humidity absorption by the films
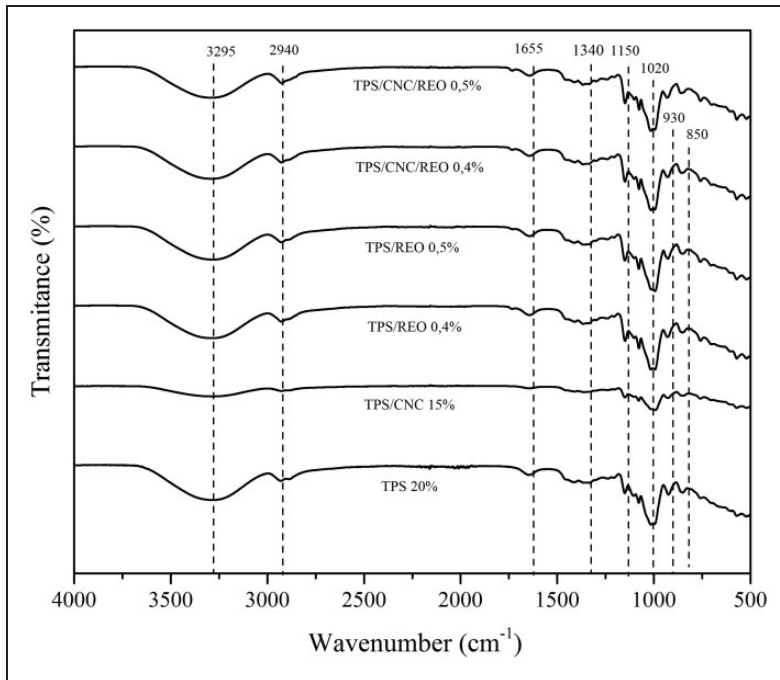
**Figure 2.** Infrared spectra of thermoplastic starch films.

formulated with these components and stored at 21°C and 55% ± 5% RH. Finally, several bands at low frequencies (less than $850\,\mathrm{cm}^{-1}$), attributed to complex modes, were observed due to vibrations in the glucose skeletal ring. Similar results were obtained by Castillo[53] and Nguyen.[5]

Thermogravimetric analysis (TGA). Table 3 presents thermogravimetric measurements to evaluate the degradation behavior of the materials (Figure 3). Thermal degradation data of the composite films are presented in Table 3.

In general, all compositions showed an initial weight loss, corresponding to the dehydration and the evaporation of glycerol up to 200°C.[40] According to Wilhelm,[54] a high moisture content (approximately 15%) in this type of material, is the result of the ease of water molecules diffusion within the matrix, due to hydrogen bonds occurring in the glycosil units.[54] During the CNC extraction, the sulfate ester groups attached to the surface of cellulose nanocrystals (CNC) might act as catalysts for thermal decomposition, resulting in a decrease in the cellulose degradation temperature. However, the CNC proportion used within the TPS matrix, did not provide an amount of sulfate ester groups enough to observe a reduction in the TPS decomposition temperature.[15] At the same time, analysis of TPS/REO and TPS/CNC/REO, as shown in Figure 3, did not lead to a significant

Table 3. Thermal transitions of the thermoplastic starch film composites.

Sample	Initial degradation temperature (°C)	Final degradation temperature (°C)	% Mass loss (volatiles)	% Mass loss at main degradation	% Residual mass at 800°C	Max dTGA (°C)
TPS 20 %	314	360	11.80	76.76	11.08	345
TPS/CNC 15 %	318	360	10.31	79.83	6.08	346
TPS/CNC/REO 0.4 %	308	360	12.58	68.94	10.20	339
TPS/CNC/REO 0.5 %	312	356	10.26	74.83	10.41	339
TPS/REO 0.4 %	315	357	9.62	78.36	9.87	339
TPS/REO 0.5 %	315	359	12.54	76.89	7.32	344
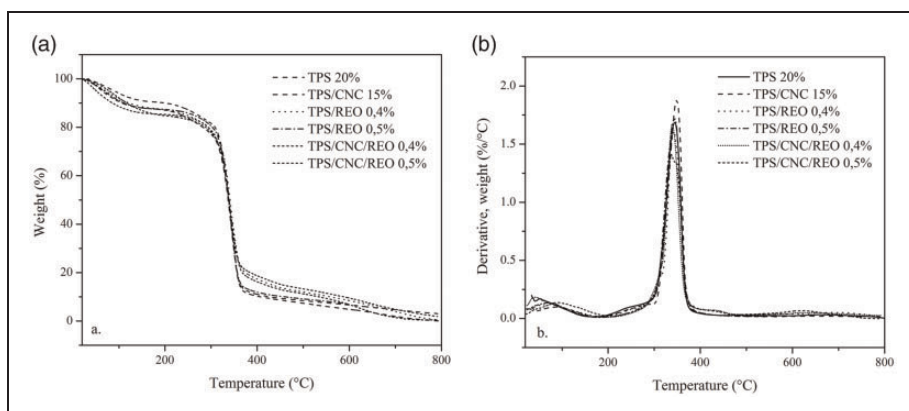
Figure 3. Thermogram (a) and derivatogram (b) of the thermoplastic starch film composites.

difference in the results when using REO within the thermoplastic matrix. However, a reduction in film thermal stability was expected because of the decrease in polymer-polymer interactions due to the presence of the essential oil. Differences in degradation temperatures can be attributed to the low REO concentration used in the TPS matrix.[15] Finally, first derivative curves for all compositions are similar, regarding all thermodegradation stages; a first event of weight loss below 200°C can be associated with the evaporation of free water and glycerol. On the other hand, a main event was observed between 339°C and 345°C, corresponding to the thermal degradation of the anhydroglucose rings of amylose and amylopectin.

Differential scanning calorimetry (DSC). Primary endothermic transitions were observed (Figure 4) due to crystal melting derived from the retrogradation process
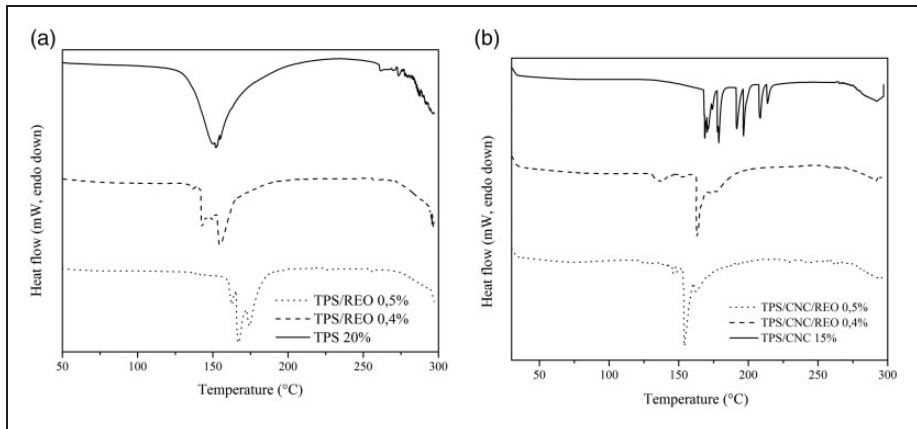
Figure 4. DSC traces of thermoplastic starch films containing (a) rosemary essential oil, and (b) cellulose nanocrystals.

that TPS undergoes after plasticization[55]; these temperatures were between 150°C and 160°C. A survey carried out by Anglès[55] showed that an increase in moisture content between 43% and 58% RH, led to an endothermic peak from 130°C to 155°C, which agrees with our results. For all films, a primary transition, attributed to the melting of crystalline amylopectin domains induced by water, could be observed. This can be ascribed to a morphological change of the gelatinized starch from an amorphous to a crystalline form occurring during storage. This event, known as retrogradation, is generated by the re-association of amylopectin in an amorphous state with a low degree of ordering, into a more orderly state. This phenomenon includes the short-range ordering formation of amylose, and the formation of double helices, distinctive of the amylopectin structure.[55]

This reorganization and crystallization of the amylopectin molecules is favored by the drying effect of the films, inducing water and glycerol release.[55] Shift of the endothermic peak towards higher temperatures in the range between 150°C and 175°C, and the formation of multiple melting peaks in various compositions, are the result of heterogeneous crystal populations.[55] In addition, TPS/CNC 15% film shows an increase in the melting temperature in the range between 150°C and 220°C caused by CNC within the matrix, and whose hydrogen bonding interactions with starch amylose and amylopectin cause a displacement towards higher temperatures, as more energy is required to melt the material.[44]

Mechanical properties. Film mechanical properties (Table 4) are related to the end-use characteristics of these materials,[23] and substantially depended on the mixture composition of starch and additives. Table 4 shows data on tensile strength for the TPS compositions; in general, tensile strength was found in the 0.50–1.80 MPa range.

Table 4. Tensile properties of the thermoplastic starch films.

Film	Tensile strength (MPa)	Elastic modulus (MPa)	Elongation at break (%)
TPS 20 %	1.26 ± 0.14	4.47 ± 0.92	76.77 ± 15.04
TPS/CNC 15 %	1.80 ± 0.11	11.95 ± 2.45	41.75 ± 4.45
TPS/REO 0.4 %	0.50 ± 0.03	2.57 ± 1.76	113.68 ± 22.90
TPS/REO 0.5 %	0.55 ± 0.05	2.64 ± 1.30	106.25 ± 25.50
TPS/CNC/REO 0.4 %	1.02 ± 0.02	5.81 ± 0.98	64.78 ± 6.94
TPS/CNC/REO 0.5 %	0.88 ± 0.08	3.50 ± 0.68	100.98 ± 9.42

These results indicated the formation of an intermolecular interaction between the starch hydroxyl group and the CNC hydroxyl group, as both structures are based on D-glucose units. Therefore, starch/CNC mixture leads to a moderate increase in tensile strength of the biocomposite films.[44] On the other hand, addition of REO yielded lower tensile strength, and higher elongation. Based on this result, it can be established that REO had a plasticizing effect, even at small concentrations.[23] These data are supported by Young modulus values, which decreased compared to non-REO compositions. Reduction in strength and stiffness could be explained mainly because of partial replacement of stronger polymer-polymer interactions with weaker polymer-oil interactions in the film network, therefore reducing cohesion of the starch network and then, film tensile strength, and matrix stiffness.[56] Likewise, TPS/CNC mechanical properties were affected by the presence of REO, that is to say, a greater amount of cellulose nanocrystal interactions was built up, thus preventing an adequate CNC dispersion within the matrix, and then reducing stiffness-tensile strength of the matrix.[44] Similar behavior was observed in cassava starch films, where the effect of adding Tween 80® as surfactant, increased free volume in the adjacent starch chains, thus generating a ductile structure.[56] It is possible to observe in Table 4 that rise in the REO proportion led to an increase in the film stretching capacity when compared to their non-REO analogs. Based on this result, it can be said that REO provides with a plasticizing effect, increasing film stretching capacity.[23]

Water interaction. Table 5 shows water interaction tests, namely solubility, permeability, and vapor transmission rate. In addition, optical properties of the thermoplastic starch films were surveyed.

   Water solubility. Solubility is a key parameter to be determined in the case of water-sensitive biopolymers such as TPS.[57] As shown in Table 5, solubility varied according to different compositions and components added to the thermoplastic

Table 5. Water interaction properties of the biocomposite films.

Film	Solubility (%)	Water vapor transmission rate (g h^{-1} m^{-2})	Water vapor permeability (g mm h^{-1} m^{-2} kPa^{-1})	Opacity (%)
TPS 20 %	6.34 ± 0.13	2.47 ± 0.05	0.144 ± 0.003	16.59 ± 0.30
TPS/CNC 15 %	4.76 ± 0.10	2.07 ± 0.01	0.121 ± 0.001	17.75 ± 0.21
TPS/REO 0.4 %	8.76 ± 0.13	3.36 ± 0.28	0.198 ± 0.016	16.24 ± 0.29
TPS/REO 0.5 %	6.07 ± 0.11	3.08 ± 0.37	0.180 ± 0.022	16.44 ± 0.30
TPS/CNC/REO 0.4 %	10.45 ± 0.11	3.37 ± 0.24	0.196 ± 0.014	17.31 ± 0.26
TPS/CNC/REO 0.5 %	9.84 ± 0.11	2.72 ± 0.31	0.158 ± 0.018	17.45 ± 0.27

matrix. Films with essential oil, regardless of the REO concentration, showed greater solubility than their non-oil analogs. This can be attributed to the fact that, despite the hydrophobic nature of the essential oils, their insertion within the polymeric matrix interferes in the polymer-polymer and polymer-CNC interactions. Therefore, insertion of water molecules within the polymer chains is facilitated, increasing film water solubility.[32] Low water solubility of the starch-based films is linked to strong intermolecular bonds between starch chains, which in turn prevent polymer dissociation. Low water solubility indicates strong interaction between starch chains; formation of hydrogen bonds between them reduces water interaction, thus reducing solubility of the polymer matrix.[17]

Permeability and water vapor transmission rate. Films capacity to delay moisture loss is an important characteristic affecting product quality.[23] Table 5 shows ranges of WVTR between 2.07 and 3.37 (g h^{-1} m^{-2}) and WVP between 0.121 and 0.198 (g mm h^{-1} m^{-2} kPa^{-1}). Regarding films containing REO, those showed higher WVP when compared with their non-REO analogs. As it can be seen in Table 5, an elevation of the rosemary oil concentration generates a decrease in WVP values. According to Shen,[58] interaction between starch and rosemary oil might prevent starch hydroxyl groups to form hydrogen bonds with water, resulting in the film WVP increase.[58]

In comparison with TPS and TPS/CNC films, no clear effects on WVP were observed in TPS/REO and TPS/CNC/REO films. Therefore, addition of REO and surfactant provided with a plasticizing effect, increasing starch chains free volume, thus favoring diffusion of water vapor.[59]

Opacity. Opacity is a material attribute that plays an important role in product packaging, because a transparent package is frequently preferred. Opacity data are presented in Table 5. Opacity values ranged from 16.24 to 17.75% for all films.

CNC-containing composites showed slightly higher opacity percentages, probably due to the formation of dense and continuous networks caused by the establishment of hydrogen bonds with CNC. Furthermore, this might lead to a partial agglomeration of CNC, unevenly dispersed in the starch-based system. Authors such as Navia[56] reported opacity from 16.4 to 16.9% for films with similar compositions using cassava starch, rosemary oil and Tween 80®. These authors established that REO and Tween80® quantities played a role to explain film opacity, as they reported an increment on such property.[23,56]

Antimicrobial activity. Antimicrobial agents can be incorporated into TPS films to provide microbiological stability, as the films can be used as carriers for a variety of additives to extend product shelf life and reduce microbial growth on food surfaces. Addition of antimicrobial agents to edible films offers advantages, such as the use of small concentrations of antimicrobials, which can be determined by establishing the minimum inhibitory concentration required to inhibit bacterial growth.[60]

Minimum inhibitory concentration. The results obtained for REO, according to the antimicrobial action spectrum proposed experimentally from 1000 to 4000 ppm (Figure 5), showed a decrease, starting at 3000 ppm in the strains of bacteria
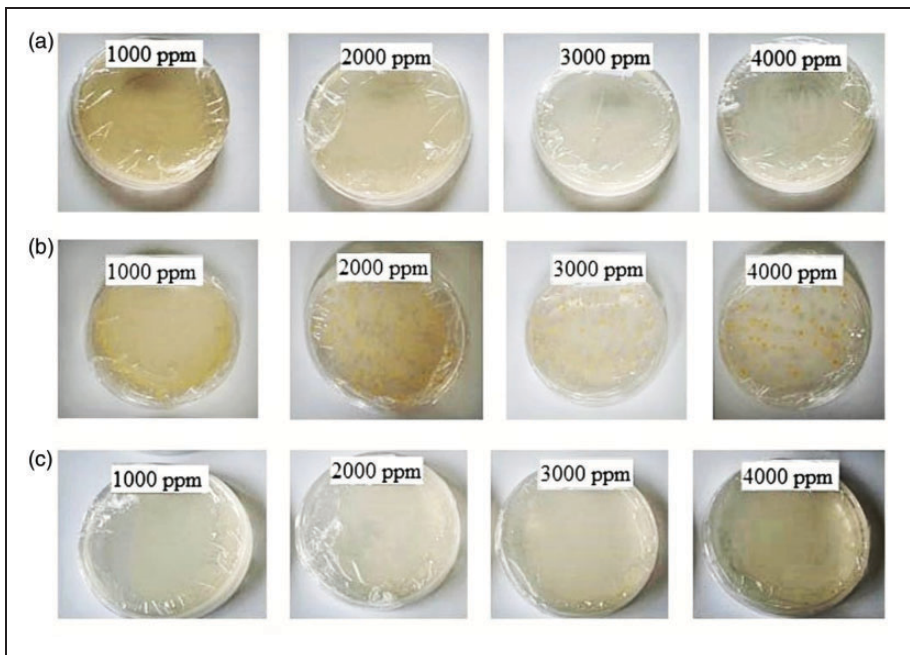

Figure 5. Rosemary essential oil minimum inhibitory concentration in *E. coli* (a), *S. Aureus* (b), and *S. enterica* (c) bacteria.

observed for the *E. coli* gram-negative. These results are consistent with findings by Castaño[34] and Mathlouthi,[61] who demonstrated the antimicrobial activity of *R. officinalis* essential oil against strains of *E. coli*; inhibition of bacterial growth was reached at a concentration of 4096 and 4400 ppm, respectively. On the other hand, REO presented antimicrobial activity against *S. aureus notorious* gram-positive starting at 2000 ppm, which is consistent with a MIC of 2048 ppm obtained by Castaño.[34] However, no inhibitory effect for the *S. enteric* gram-negative bacteria could be observed under any concentration in the antimicrobial action spectrum proposed in our research.

The inhibition spectrum against REO extract can be explained based on the potential damage mechanisms on the bacterial cell membrane, due to the permeability increase and its structural impact.[34] REO antimicrobial mode of action is considered to arise primarily from its hydrophobic potential to enter the bacterial cell membrane, disintegrate membrane structures, cause ion leakage, and/or interact with intracellular sites critical to bacterial activities. Specifically, they can inhibit the activity of the glucosyltransferase enzyme, which is responsible for the adhesion of bacteria to their sites.[61] Furthermore, it has been established that the hydrophilic structure of the cell wall of gram-negative bacteria, consisting essentially of a lipopolysaccharides, blocks the penetration of oil hydrophobic components, which helps explain why gram-positive bacteria are more sensitive to the effects of essential oils.[60] A research conducted by Klancnik,[62] revealed that the *S. enterica* gram-negative bacteria exhibited noticeable resistance to REO extracts, as the outer membrane surrounding the cell wall in gram-negative bacteria, prevents compound diffusion through its lipopolysaccharide layer.

The chemical composition of essential oils is critical to their antibacterial function.[34] Several studies have been carried out to determine whether the antibacterial activity of essential oils could be related to their main compounds; α-pinene, myrcene, 1,8-cineole, camphor and borneol. In addition, other minor components have also been reported for their antimicrobial activity, such as β-pinene, limonene, α-terpene and camphene.[60] Minor components are critical to antibacterial activity, and can have potential influence.[33] For this purpose, antibacterial activity of these compounds has been evaluated under same experimental conditions; data shown by Ojeda-Sana[60] demonstrate that α-pinene was the only compound capable of inhibiting all the microorganisms tested, including *S. aureus* and *E. coli,* and MIC from 800 to 8000 ppm. On the other hand, camphor and borneol only inhibited gram-positive bacteria, while 1,8-cineole was active against gram-negative bacteria, with MIC values ranging from 8000 to 20000 ppm.[60]

Regarding to the antifungal activity results shown in Figure 6, REO tested on potato dextrose agar plates exhibited an effective inhibitory effect against all fungi experimentally analyzed, with a MIC of 4000 ppm for *A. flavus* and *A. niger*, and 3000 ppm for *F. oxyporum*. These results are consistent with De Souza,[33] who confirmed the antimicrobial activity for *Aspergillus niger* and *Aspergillus flavus* fungi. Researchers such as Özcan,[48] have studied the effectiveness of REO in fungus growth, concluding that main substances such as thymol, carvacrol and
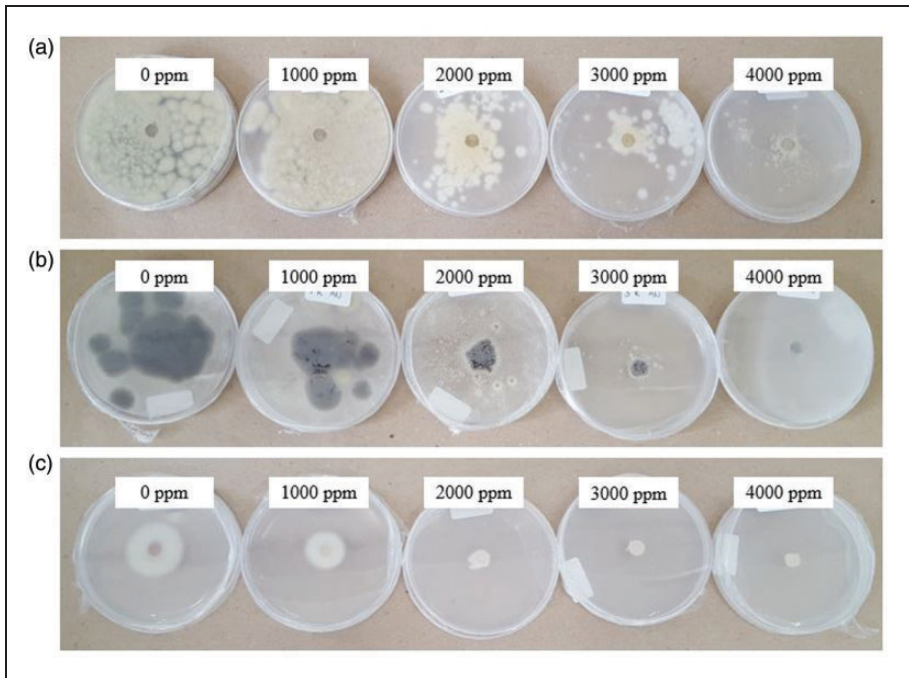
Figure 6. Rosemary essential oil minimum inhibitory concentration in *A. flavus* (a), *A. niger* (b), and *F. oxyporum* (c) fungi, in REO concentrations (0, 1000, 2000, 3000, 4000) ppm, (from left to right).

menthol, are responsible for the antifungal effect. Therefore, the results suggest the potential use of some oils as antifungal food preservatives. Although high levels of volatile oils can adversely affect the sensory properties of foods, lowest concentrations may suffice for food safety purposes in real-world situations where microbial loads are low.[48]

Differences in microorganism susceptibility could be attributed to the variation in sample penetration rate through the cell wall and cell membrane structures, as well as their adaptation response and survival strategy derived from their species.[36] In addition, various antimicrobial activity reviews on essential oils have reported multiple factors, ranging from plant cultivation to variants in experimental conditions for measuring antibacterial activity, as well as methodology differences affecting the diversity of experimental results.[22,60]

Qualitative disk inhibition test. The growth of spoilage microorganisms and foodborne pathogens is one of the most important causes in food degradation. The presence of food spoilage microorganisms can accelerate lipid oxidation and other oxidation processes and change food organoleptic properties. Foodborne pathogens are directly responsible for certain human diseases, or indirectly
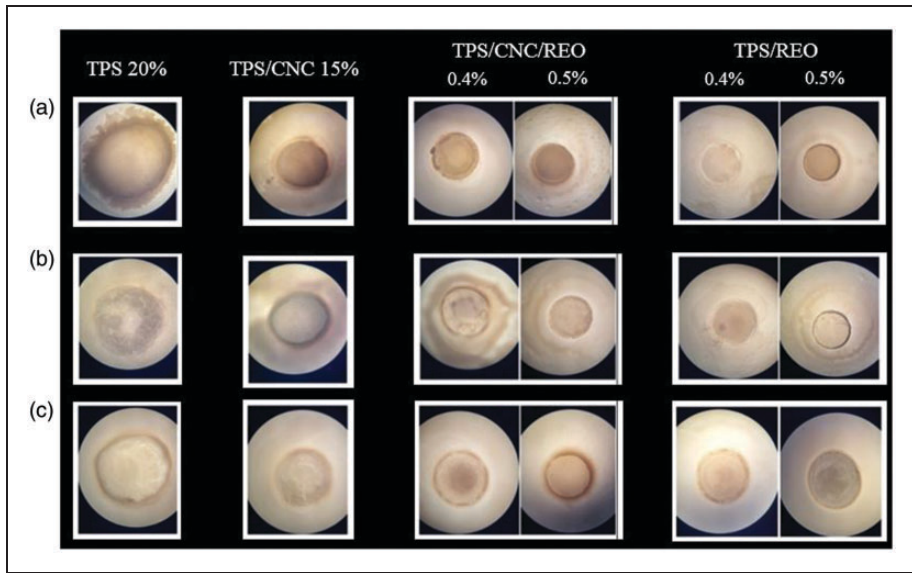
Figure 7. Disk inhibition test in thermoplastic starch films with *E. coli* (a), *S. Aureus* (b), *and S. enterica* (c) bacteria.

responsible due to toxin production.[23] Determination of the antimicrobial activity of TPS biocomposites based on various CNC and REO contents was studied versus three common food poisoning bacteria; *E.coli, S. Aureus,* and *S. enterica*, as summarized in Figure 7, and three common food environment fungi; *A. flavus, A. niger,* and *F. oxysporum*, as seen in Figure 8. Considering the non-antimicrobial character of the starch and other components present in the filmogenic solution, the TPS 20% and TPS/CNC 15% films did not show any antimicrobial activity against the bacteria and fungi.

On the other hand, the disk inhibition test for REO in the case of TPS/CNC/REO 0.4 and 0.5% films, showed a zone of inhibition in both compositions for *E. coli* bacteria, while a zone of inhibition was observed for the *S. Aureus* bacteria only in the TPS/CNC film with a 0.5% REO content. However, no inhibition effect could be observed for *S. enterica* bacteria in the films. Regarding the results from the disk inhibition test carried out on fungi for TPS/CNC/REO compositions, a decrease in sporulation was observed with *A. niger* fungus, with a small zone of inhibition around the film with 0.5% REO content. In the case of *A. flavus* and *F. oxysporum* fungi, no decrease in sporulation could be observed around the TPS disks.

Regarding 0.4 and 0.5% TPS/REO films, results revealed zones of inhibition for each of the bacteria according to the zone diameter observed in the film with 0.5% REO content in the following order: *E. coli* > *S. enterica* > *S. Aureus*. On the other hand, TPS/REO film compositions showed antifungal activity mainly for *A. niger*
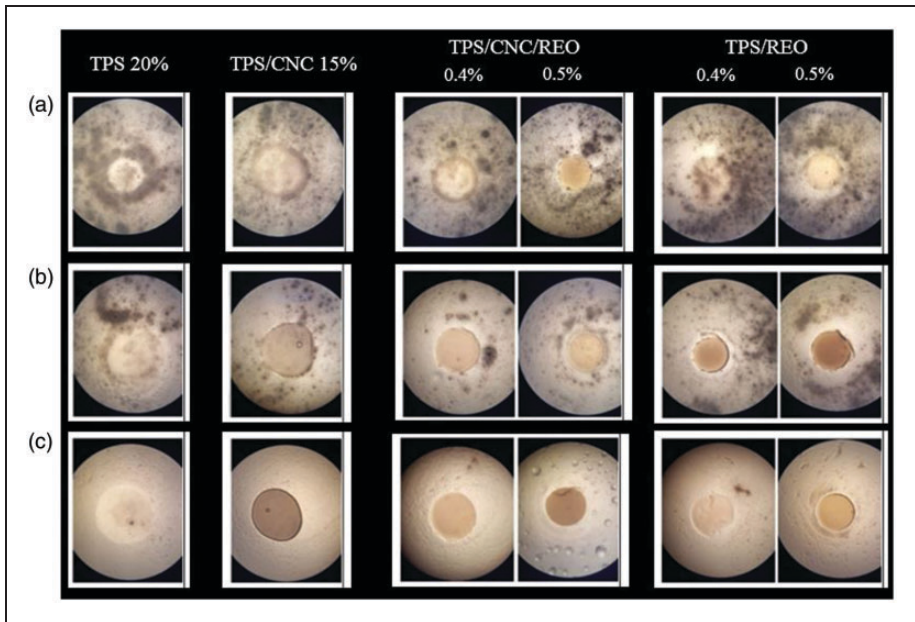
Figure 8. Disk inhibition test in thermoplastic starch films with A. flavus (a), A. niger (b), and F. oxysporum (c) fungi.

fungus for both REO concentrations, most noticeably 0.5% REO. As for *A. falvus* fungus, there was a decrease in fungal sporulation, however, no zone of inhibition could be observed. Finally, for *F. oxysporum* fungus, a small zone of inhibition around the film was identified with 0.5% REO. Films with antibacterial activity showed greater performance, when increasing REO concentration from 0.4 to 0.5%. In general, incorporation of essential oils into edible films through vapor phase requires smaller concentrations, as compared to those required in a direct application of the essential oil in food, therefore inhibiting different types of microorganisms.[30] This result confirms that REO can successfully act as an antimicrobial agent in combination with a TPS, TPS/CNC/REO and TPS/REO biocomposite films; the inhibitory action will depend on the concentration within the thermoplastic film for the development of an active packaging material. The antimicrobial analysis was useful in evaluating the inhibition of fungi by volatile REO compounds and comparing the capacities of different fungal spores to colonize the surfaces of the biocomposite films. Exposure to volatile compounds of essential oils leads to alterations in the morphology of hyphae, which can be linked to the effect of essential oils in the enzymatic reactions regulating wall synthesis.

The lipophilic properties of the oil components also contribute to the REO capacity to penetrate the plasma membrane.[30]

Conclusions and recommendations

Starch was successfully plasticized with water and glycerol in the presence of CNC and REO. Mechanical properties of the TPS films were greatly affected by the added emulsifier when REO was used. TPS film containing 15% CNC offered best performance in terms of tensile strength and water interaction, lowest solubility, permeability and water vapor transmission rate. Rosemary oil influenced on the inhibition of food-related pathogenic microorganisms, revealed action against *E. coli* and *S. aureus* bacteria and the *A. niger* fungus. *S. enterica* bacteria exhibited a noticeable resistance to the diffusion of REO components restricted by the cell wall outer membrane in gram-negative bacteria. TPS composites containing REO are potential bioactive films that can extend food product shelf life, without significantly affecting properties such as transparency. However, these applications still require more research on the migration phenomena to ensure better control of the food organoleptic properties. Also additional research is necessary to keep some of the good mechanical qualities of the starch, even in presence of plasticizing or emulsifying agents.

ORCID iD

Guillermo Jimenez https://orcid.org/0000-0002-6369-5239

References

1. Pelissari FM, Andrade-Mahecha MM, Sobral Pj do A, et al. Nanocomposites based on banana starch reinforced with cellulose nanofibers isolated from banana peels. *J Colloid Interface Sci* 2017; 505: 154–167.
2. Oriani VB, Molina G, Chiumarelli M, et al. Properties of cassava starch-based edible coating containing essential oils. *J Food Sci* 2014; 79: 189–194.
3. Llanos JHR and Tadini CC. Preparation and characterization of bio-nanocomposite films based on cassava starch or chitosan, reinforced with montmorillonite or bamboo nanofibers. *Int J Biol Macromol* 2018; 107: 371–382.
4. López-Córdoba A, Medina-Jaramillo C, Piñeros-Hernandez D, et al. Cassava starch films containing rosemary nanoparticles produced by solvent displacement method. *Food Hydrocoll* 2017; 71: 26–34.
5. Nguyen Vu HP and Lumdubwong N. Starch behaviors and mechanical properties of starch blend films with different plasticizers. *Carbohydr Polym* 2016; 154: 112–120.
6. Zhu F. Composition, structure, physicochemical properties, and modifications of cassava starch. *Carbohydr Polym* 2015; 122: 456–480.
7. Souza AC, Goto GEO, Mainardi JA, et al. Cassava starch composite films incorporated with cinnamon essential oil: antimicrobial activity, microstructure, mechanical and barrier properties. *LWT – Food Sci Technol* 2013; 54: 346–352.
8. Rajaei A, Tabatabaei M and Mohsenifar A. Physical and antimicrobial properties of starch-carboxy methyl cellulose film containing rosemary essential oils encapsulated in chitosan nanogel. *Int J Bio Macromol* 2018; 112: 148–155.
9. Kim S, Yang S, Chun HH, et al. High hydrostatic pressure processing for the preparation of buckwheat and tapioca starch films. *Food Hydrocoll* 2018; 81: 71–76.
10. Xie F, Pollet E, Halley PJ, et al. Starch-based nano-biocomposites. *Prog Polym Sci* 2013; 38: 1590–1628.
11. Ma X, Chang PR and Yu J. Properties of biodegradable thermoplastic pea starch/carboxymethyl cellulose and pea starch/microcrystalline cellulose composites. *Carbohydr Polym* 2008; 72: 369–375.
12. De Azeredo HMC. Nanocomposites for food packaging applications. *Food Res Int* 2009; 42: 1240–1253.
13. Babaee M, Jonoobi M and Hamzeh Y. Biodegradability and mechanical properties of reinforced starch nanocomposites using cellulose nanofibers. *Carbohydr Polym* 2015; 132: 1–8.
14. Kalia S, Dufresne A, Cherian BM, et al. Cellulose-based bio- and nanocomposites: a review. *Int J Polym Sci* 2011; 2011: 1–35.
15. González K, Retegi A, González A, et al. Starch and cellulose nanocrystals together into thermoplastic starch bionanocomposites. *Carbohydr Polym* 2015; 117: 83–90.
16. Khalid S, Yu L, Feng M, et al. Development and characterization of biodegradable antimicrobial packaging films based on polycaprolactone, starch and pomegranate rind hybrids. *Food Packag Shelf Life* 2018; 18: 71–79.
17. Luchese CL, Spada JC and Tessaro IC. Starch content affects physicochemical properties of corn and cassava starch-based films. *Ind Crops Prod* 2017; 109: 619–626.
18. Dvaranauskaite A, Venskutonis PR, Raynaud C, et al. Variations in the essential oil composition in buds of six blackcurrant (Ribes nigrum L) cultivars at various development phases. *Food Chem* 2009; 114: 671–679.

19. Wannes WA, Mhamdi B, Sriti J, et al. Antioxidant activities of the essential oils and methanol extracts from myrtle (Myrtus communis var italica L) leaf, stem and flower. *Food Chem Toxicol* 2010; 48: 1362–1370.

20. Hill LE, Gomes C and Taylor TM. Characterization of beta-cyclodextrin inclusion complexes containing essential oils (trans-cinnamaldehyde, eugenol, cinnamon bark, and clove bud extracts) for antimicrobial delivery applications. *LWT - Food Sci Technol* 2013; 51: 86–93.

21. Costa DC, Costa HS, Albuquerque TG, et al. Trends in food science and technology advances in phenolic compounds analysis of aromatic plants and their potential applications. *Trends Food Sci Technol* 2015; 45: 336–354.

22. Santos RR, Costa DC, Cavaleiro C, et al. A novel insight on an ancient aromatic plant: the rosemary (Rosmarinus officinalis L). *Trends Food Sci Technol* 2015; 45: 355–368.

23. Atarés L and Chiralt ASC. Essential oils as additives in biodegradable films and coatings for active food packaging. *Trends Food Sci Technol* 2016; 48: 51–62.

24. Dannenberg S, Funck GD, Eduardo C, et al. Essential oil from pink pepper as an antimicrobial component in cellulose acetate film: potential for application as active packaging for sliced cheese. *LWT – Food Sci Technol* 2017; 81: 314–318.

25. Moura MRD, Mattoso LHC and Zucolotto V. Development of cellulose-based bactericidal nanocomposites containing silver nanoparticles and their use as active food packaging. *J Food Eng* 2012; 109: 520–524.

26. Adilah AN, Jamilah B, Noranizan MA, et al. Utilization of mango peel extracts on the biodegradable films for active packaging. *Food Packag Shelf Life* 2018; 16: 1–7.

27. Kaushik A and Tiwari SK. Evaluation of antimicrobial activity and phytochemical analysis of citrus Limon. *J Agric Chem Biotechnol* 2011; 5: 43–56.

28. Qin Y, Li W, Liu D, et al. Development of active packaging film made from poly (lactic acid) incorporated essential oil. *Prog Org Coat* 2017; 103: 76–82.

29. Ribeiro-Santos R, Andrade M and Sanches-Silva A. Application of encapsulated essential oils as antimicrobial agents in food packaging. *Curr Opin Food Sci* 2017; 14: 78–84.

30. Avila-Sosa R, Palou E, Jiménez Munguía MT, et al. Antifungal activity by vapor contact of essential oils added to amaranth, chitosan, or starch edible films. *Int J Food Microbiol* 2012; 153: 66–72.

31. Ghasemlou M, Aliheidari N, Fahmi R, et al. Physical, mechanical and barrier properties of corn starch films incorporated with plant essential oils. *Carbohydr. Polym* 2013; 98: 1117–1126.

32. Amaral J, Dannenberg S, Biduski B, et al. Antibacterial activity, optical, mechanical, and barrier properties of corn starch films containing orange essential oil. *Carbohydr Polym* 2019; 222: 114981.

33. De Sousa LL, De Andrade SCA, Athayde AJAA, et al. Efficacy of Origanum vulgare L. and Rosmarinus officinalis L. essential oils in combination to control postharvest pathogenic aspergilli and autochthonous mycoflora in Vitis labrusca L. (table grapes). *Int J Food Microbiol* 2013; 165: 312–318.

34. Castaño P, Ciro G, Zapata M, et al. Actividad bactericida del extracto etanólico y del aceite esencial de hojas de rosmarinus officinalis l sobre algunas bacterias de interés alimentario. *Vitae* 2010; 17: 149–154.

35. Montero-Recalde MA, Martinez-Jimenez JA, Aviles-Esquivel DF, et al. Effect antimicrobial of extract of rosmarinus officinalis on strain of escherichia coli. *J Selva Andina Biosph* 2017; 5: 168–175.

36. Jiang Y, Wu N, Fu Y, et al. Chemical composition and antimicrobial activity of the essential oil of rosemary. *Environ Toxicol Pharmacol* 2011; 32: 63–68.

37. Dos Santos RM, Flauzino Neto WP, Silvério HA, et al. Cellulose nanocrystals from pineapple leaf, a new approach for the reuse of this agro-waste. *Ind Crops Prod* 2013; 50: 707–714.

38. Conde-Hernández LA, Espinosa-Victoria JR, Trejo A, et al. CO2-Supercritical extraction, hydrodistillation and steam distillation of essential oil of rosemary (Rosmarinus officinalis). *J Food Eng* 2017; 200: 81–86.

39. Erkan N, Ayranci G and Ayranci E. Antioxidant activities of rosemary (Rosmarinus officinalis L.) extract, blackseed (Nigella sativa L.) essential oil, carnosic acid, rosmarinic acid and sesamol. *Food Chem* 2008; 110: 76–82.

40. López OV, Ninago MD, Lencina MMS, et al. Thermoplastic starch plasticized with alginate-glycerol mixtures: melt-processing evaluation and film properties. *Carbohydr Polym* 2015; 126: 83–90.

41. Ghanbari A, Tabarsa T, Ashori A, et al. Preparation and characterization of thermoplastic starch and cellulose nanofibers as green nanocomposites: extrusion processing. *Int J Biol Macromol* 2018; 112: 442–447.

42. Savadekar NR and Mhaske ST. Synthesis of nano cellulose fibers and effect on thermoplastics starch based films. *Carbohydr Polym* 2012; 89: 146–151.

43. American Society for Testing and Materials. *Designation: D882 – 18: 'Standard test method for tensile properties of thin plastic sheeting'*. West Conshohocken: American Society for Testing and Materials, 2018, pp. 1–13.

44. Ma X, Cheng Y, Qin X, et al. Hydrophilic modification of cellulose nanocrystals improves the physicochemical properties of cassava starch-based nanocomposite films. *LWT - Food Sci Technol* 2017; 86: 318–326.

45. Daudt RM, Avena-Bustillos RJ, Williams T, et al. Comparative study on properties of edible films based on pinhão (Araucaria anogustifolia) starch and flour. *Food Hydrocoll* 2016; 60: 279–287.

46. Ribeiro-Santos R, Andrade M, Ramos N, et al. Biological activities and major components determination in essential oils intended for a biodegradable food packaging. *Ind Crop Prod* 2017; 97: 201–210.

47. Stojanović-Radić Z, Pejčić M, Joković N, et al. Inhibition of salmonella enteritidis growth and storage stability in chicken meat treated with basil and rosemary essential oils alone or in combination. *Food Control* 2018; 90: 332–343.

48. Özcan MM and Chalchat JC. Chemical composition and antifungal activity of rosemary (Rosmarinus officinalis L.) oil from Turkey. *Int J Food Sci Nutr* 2008; 59: 691–698.

49. Jalali-Heravi M, Moazeni RS and Sereshti H. Analysis of Iranian rosemary essential oil: application of gas chromatography-mass spectrometry combined with chemometrics. *J Chromatogr A* 2011; 1218: 2569–2576.

50. Proestos C, Lytoudi K, Mavromelanidou OK, et al. Antioxidant capacity of selected plant extracts and their essential oils. *Antioxidants* 2013; 2: 11–22.

51. Hesenov A and Erbatur O. Study on the stability of supercritical fluid extracted rosemary (Rosmarinus offcinalis L.) essential oil. *J Anal Chem* 2010; 65: 899–906.

52. Yeşilbag D, Eren M, Agel H, et al. Effects of dietary rosemary, rosemary volatile oil and vitamin E on broiler performance, meat quality and serum SOD activity. *Br Poult Sci* 2011; 52: 472–482.

53. Castillo L, López O, López C, et al. Thermoplastic starch films reinforced with talc nanoparticles. *Carbohydr Polym* 2013; 95: 664–674.
54. Wilhelm H, Sierakowski M, Souza GP, et al. Starch films reinforced with mineral clay. *Carbohydr Polym* 2003; 52: 101–110.
55. Anglès MN and Dufresne A. Plasticized starch/tunicin whiskers nanocomposites. 1. Structural analysis. *Macromol* 2000; 33: 8344–8353.
56. Navia Porras DP, Gordillo Suárez M, Hernández Umaña J, et al. Optimization of physical, optical and barrier properties of films made from cassava starch and rosemary oil. *J Polym Environ* 2019; 27: 127–140.
57. Basiak E, Lenart A and Debeaufort F. Effect of starch type on the physico-chemical properties of edible films. *Int J Biol Macromol* 2017; 98: 348–356.
58. Shen XL, Wu JM, Chen Y, et al. Antimicrobial and physical properties of sweet potato starch films incorporated with potassium sorbate or chitosan. *Food Hydrocoll* 2010; 24: 285–290.
59. Brandelero RPH, Yamashita F and Grossmann MVE. The effect of surfactant tween 80 on the hydrophilicity, water vapor permeation, and the mechanical properties of cassava starch and poly (butylene adipate-co-terephthalate) (PBAT) blend films. *Carbohydr Polym* 2010; 82: 1102–1109.
60. Ojeda-Sana AM, van Baren CM, Elechosa MA, et al. New insights into antibacterial and antioxidant activities of rosemary essential oils and their main components. *Food Control* 2013; 31: 189–195.
61. Mathlouthi N, Bouzaienne T, Oueslati I, et al. Use of rosemary, oregano, and a commercial blend of essential oils in broiler chickens: in vitro antimicrobial activities and effects on growth performance. *J Anim Sci* 2012; 90: 813–823.
62. Klancnik A, Guzej B, Kolar MH, et al. In vitro antimicrobial and antioxidant activity of commercial rosemary extract formulations. *J Food Prot* 2009; 72: 1744–1752.

Author Biographies

Josette Araya studied Industrial Chemistry at the Universidad Nacional, Heredia, Costa Rica where she obtained her B. Sc. Her research thesis was on thermoplastic starch from cassava filled with nanocellulose from pineapple. In 2019 she did a research stay at the Universidad de San Buenaventura, Cali, Colombia.

Marianelly Esquivel studied Industrial Chemistry at the Universidad Nacional, Heredia, Costa Rica, where she earned her B. Sc. Then, she moved to Guadalajara, Mexico, where she obtained a M. Sc. on paper and cellulose. She works at the Laboratory of Polymers, School of Chemistry, Universidad Nacional, Heredia, Costa Rica. Her main interests are cellulose, nanocellulose, and lignocellulosic fibers.

Guillermo Jimenez studied Chemistry at the Universidad de Costa Rica, San Jose, Costa Rica, where he obtained his B.Sc. He obtained a M.Sc. in Polymer Engineering at the Tokyo Institute of Technology, Tokyo, Japan, and a Ph. D. in Polymer Engineering at the University of Akron, Ohio, U.S.A. He works at the Laboratory of Polymers, School of Chemistry, Universidad Nacional, Heredia,

Costa Rica. His main interests are polymer composites and nanocomposites, nano-cellulose, and starch.

Diana Navia obtained her B. Sc. in Agro-industrial Engineering at the Universidad del Cauca, Popayan, Colombia, and studied Food Engineering at the Universidad del Valle, Cali, Colombia where she earned her M. Sc. and Ph.D. degrees. She has done research on semi-rigid and flexible starch-based bioplastics since 2008, holding 4 patents, 3 book chapters, and 22 scientific papers on the subject. She has more than 10 years as professor, and currently works at the Universidad de San Buenaventura, Cali, Colombia.

Luis Poveda obtained B. Sc. in Agro-Industrial Engineering, and M. Sc. in Biotechnology Engineering at the Universidad de San Buenaventura, Cali, Colombia, where he currently works as a researcher and professor. He is interested in agro-industrial food products design, agro-industrial residues, functional foods design, and bioplastics development.